ISTITUTO NAZIONALE DI FISICA NUCLEARE

Sezione di Milano

INFN/TC-84/13
13 Luglio 1984

N.Croitoru, P.G.Rancoita and A.Seidman :

CHARGE MIGRATION CONTRIBUTION TO THE SENSITIVE LAYER OF A SILICON DETECTOR

Servizio Documentazione
dei Laboratori Nazionali di Frascati

Istituto Nazionale di Fisica Nucleare
Sezione di Milano

INFN/TC-84/13
13 Luglio 1984

CHARGE MIGRATION CONTRIBUTION TO THE SENSITIVE LAYER OF A SILICON DETECTOR

N.Croitoru(x), P.G.Rancoita and A.Seidman(x)

ABSTRACT

The charge migration from the field-free region has been investigated, by comparing the expected peak position (which takes into account the depleted layer only) of the energy-loss of relativistic electrons with the measured one. The measured sensitive layer was found to be systematically larger than the depleted one. This effect is accounted for the charge migration due to diffusion.

1.- INTRODUCTION

Silicon detectors are currently a major instrument in high-energy physics experiments (for a review on the subject see Refs.(1) and (2)). They are attractive as inner vertex detectors and as electromagnetic calorimeters in colliding beam machine experiments. However in the latter case very large areas are required. In calorimetry the active volume can be small and, therefore, relatively low resistivity undepleted (not fully depleted) devices can be used[3-5]. The associated electronics is supposed to be operated with long-integration times. Therefore hole-electron pairs generated on the passage of relativistic particles in the field free region can be collected due to charge diffusion.

This paper presents an investigation of the charge migration effect from the field free region of silicon detectors operating undepleted. Both the electron and hole contributions are considered.

(x) Tel-Aviv University, Ramat-Aviv, Israel.

2.- CHARGE COLLECTION FROM THE FIELD FREE REGION

In a solid state device operating not fully depleted (Fig.1) the overall sensitive region is provided by a charge-depleted layer $X_d = X_n + X_p$ and an additional zone, $X_M = X_{Mh} + X_{Me}$, of the field free region,

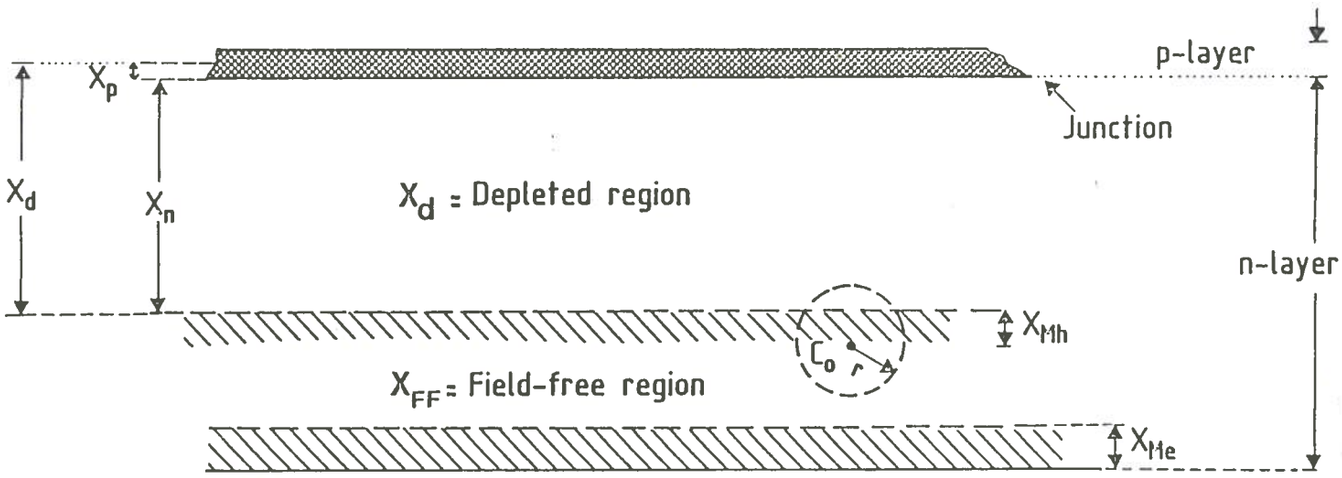

FIG. 1 - Sectional view of an undepleted n-type bulk silicon detector.

where X_{Me} is the layer from which electrons migrate towards the positive electrode and X_{Mh} is the layer from which the holes migrate into the space-charge layer. The time interval of the charge-collection, which determines the value of X_M, is defined by the associated electronics, therefore it can be arranged to be a fraction of a carrier-diffusion length. The carrier diffusion equation is

$$\partial c'/\partial t = -c'/\tau_c + D \nabla^2 c' \qquad (1)$$

where c' is the excess carrier concentration to thermal equilibrium, τ_c is the carrier lifetime, D[6] is the carrier diffusion coefficient, D_n for electrons and D_p for holes. However, if a large number of minority carriers are injected into a semiconductor, i.e. $n \approx p$ in the injection region, the density of the majority carriers will also be affected. In this case, the minority carrier diffusion coefficient (i.e. the hole diffusion coefficient in a n-type bulk silicon) has to be replaced by an ambipolar diffusion coefficient

$$D_{amb} = 2 D_n D_p / (D_n + D_p) .$$

For silicon at 300K, D_{amb} is about 18 cm^2/sec, where $D_n \approx 35$ and $D_p \approx 12$ cm^2/sec. For relativistic particles traversing a detector, the density of the generated carriers along the particle path (about 80 e-h/μm) modifies the equilibrium carrier concentration, like in the case of high injection. This high-injection state occurs only for a few nanoseconds after the particle passage. During this time duration the carrier diffusion coefficients are replaced by the ambipolar diffusion coefficient.

The solution of eq.(1) provides the transient of the carrier excess in a unit-volume at a distance r from the position where C_o charges were created at t = 0. For a collection time[7] $\tau < \tau_c$

$$c'(\tau,r)dV = C_o \exp(-r^2/2\sigma^2) / [(2\pi)^{3/2} \sigma^3] r^2 dr d\Omega \qquad (2)$$

where $\sigma = \sqrt{(2D\tau)}$ and Ω is the solid angle.

The probability that an electron created in X_{Me} and a hole in X_{Mh} at a distance r from the respective limits of the field-free region (Fig.1) are collected, can be calculated from eq.(2).

3.- EXPERIMENTAL MEASUREMENTS

In the present investigation, the energy-loss of relativistic β^-, from a Ru_{106} source, has been measured for two devices operated both as fully depleted and undepleted detectors. This way the contribution of the field free region to the overall sensitive layer was determined.

These detectors, N6 and A[8], are of high resistivity (about 8 and 40 kΩcm) and low leakage current (about 25 and 40 nA, respectively).

3.1.- Depleted layer depth

The width of the depleted layer in an abrupt junction in the n-type silicon, X_n, is given as

$$X_n \approx \sqrt{(2\,\varepsilon_{Si}\,\varepsilon_o\,\mu_n\,\varrho\,[V + V_B])} \qquad (3)$$

where ϱ is the resistivity, V is the external applied reverse bias, ε_o is the free space permittivity and ε_{Si} is the dielectric constant of silicon. For $V \gg V_B$, $X_n \approx 0.529\times10^{-4}\cdot\sqrt{(\varrho V)}$ cm . The built-in voltages, V_B, for both detectors were found to be lower than 0.3 V.

The corresponding depletion layer capacitance per unit-area, C_T, for this junction is

$$C_T = \varepsilon_{Si}\,\varepsilon_o/X_d \approx 1.0359\times10^{-12}/X_d \quad (Fcm^{-2}) \; . \qquad (4)$$

From eq.(3) and assuming $X_d \approx X_n$ in eq.(4)

$$C_T \approx 1.958\times10^{4}/\sqrt{(\varrho V)} \qquad (pFcm^{-2}) \; . \qquad (5)$$

In Fig.2, the capacitance as a function of the applied dc bias voltage for detectors N6 and A are shown. Measurements were performed using a Boonton, Model 72B capacitance meter (at an ac signal of

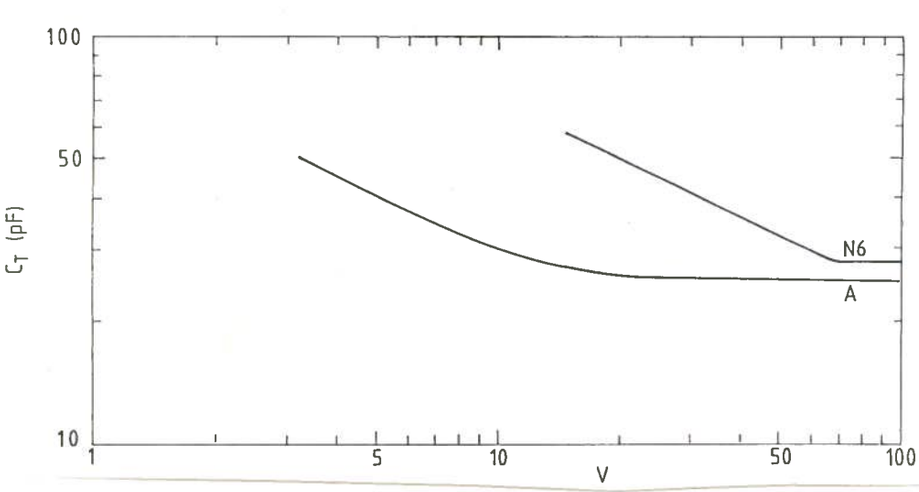

FIG. 2 - Capacitance vs applied reverse bias voltage.

15 mV and 1 MHz). They are consistent with the square root behaviour presented by eq.(5). By measuring the capacitance and using eq.(4) the depletion region X_d is determined with an accuracy of $\approx 0.7\%$.

The actual sensitive layer X_d+X_M was found by comparing data of the energy loss of charged particles from undepleted with those of fully depleted detectors.

3.2.- Experimental set-up

A Ru_{106} β^- source of 4 mm diameter was located at 3.5 cm from the silicon device, Si, namely N6 or A, under measurement (Fig. 3). Downstream, another silicon detector, Si_B (300 μm thick), an Al absorber (200 μm thick) and a scintillator Sc (3mm thick) were positioned. The active areas of these devices were 1 cm^2.

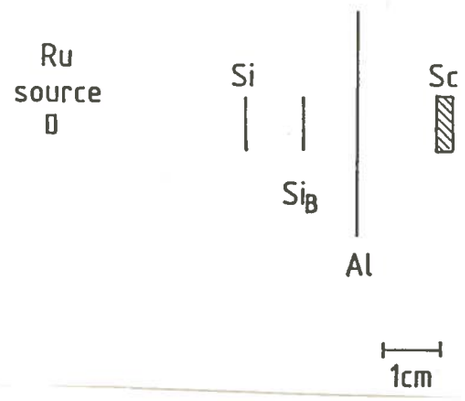

FIG. 3 - Experimental lay-out. The detector under measurement, i.e. N6 or A, is indicated by Si.

The signal pulses from the silicon detectors were sent to standard ORTEC-125 charge preamplifiers. The preamplified signals went to ORTEC-472 spectroscopy amplifiers. The output pulse from the amplifier associated to Si_B had a rise-time of about 0.4 μs and a base-time of about 1.2 μs. The threshold of the associated discriminator was set to a value slightly lower than the corresponding signal of a minimum ionizing particle traversing Si_B. Two photomultipliers were coupled to the Sc device. Their output pulses were sent to discriminators and set coincidences, which gave a 40 ns wide signal.

The trigger was defined by the coincidence of the Si_B detector and the scintillator Sc (the latter generating a jitter of only a few ns). The trigger signal provided a gate for a peak sensing LeCroy 2259 ADC, where the pulse coming from the upstream detector was recorded and subsequently read out by an HP 2100 computer. The gate widths were set 0.7, 1.2 and 3.0 μs for corresponding shaping times 0.5, 1.0 and 2.0 μs of the amplifier associated to Si. The counting rate was about 30 triggers s^{-1}.

The detector Si together with its associated electronics has a gaussian noise distribution, σ_{noise}, whose typical value was 5.1 ± 0.5 keV. The exact value was determined separately for each data taking. The Si detector had the negative bias applied to the junction side.

The above described arrangement selected electrons emitted in a forward cone of $\pm 4^o$, with an initial kinetic energy greater than 0.8 MeV ($\beta > 0.92$). Thus, the overall energy-loss spectra are described, to a first approximation, by a Landau distribution convolved by a gaussian function. The standard deviation of the convolving normal function takes into account both the noise contribution and the effect of atomic electron binding energies[9].

4.- DETERMINATION OF THE CHARGE MIGRATION EFFECT

The energy-loss of a relativistic particle (in this case electrons with $\beta > 0.92$) is proportional[10] to the thickness x of the traversed absorber. A measurement of the most probable energy-loss, in the detector Si, determines the overall sensitive layer $X = X_d+X_M$. The depleted layer X_d is measured independently by the detector capacitance (Sect. 3.1). Thus the evaluation of the field free region contribution, X_M, to the overall charge collection is possible.

4.1.- Energy-loss of Ru β^-

Electrons having kinetic energies between 0.8 and 3 MeV (as for β^- emitted by a Ru source) loose energy mostly by collision. The critical energy, namely the energy at which the collision loss is equal to the radiation loss, is about 52.6 MeV in a silicon absorber. The radiation loss is about 2.6% of the total energy-loss at 3.0 MeV and about 0.7% at about 0.8 MeV[11]. In the following discussion the radiation loss is neglected.

The electron stopping power is calculated to Bethe's stopping theory, as formulated by Rohrich and Carlson[12]

$$d\varepsilon/dx = (\xi/x)\{\ln[\eta^2(\eta+2)/(2(I/m_e c^2)^2)] + F(\eta) - \delta\} \qquad (6)$$

where η is the electron kinetic energy in units of $m_e c^2$, I is the mean excitation energy ($\simeq 172$ eV in Si and

$$\xi = (2\pi e^4/2m_e c^2\beta^2)N_A Z \times \varrho/A$$

m_e is the electron mass, N_A is the Avogadro number, Z, A and ϱ are, correspondingly, the atomic number, the atomic weight and the density of the material and x is the traversed thickness in cm; $\xi = 0.179x/\beta^2$ (MeV) for Si absorber and β_c is the velocity of the incoming electron

$$F(\eta) = 1 - \beta^2 + [\eta^2/8 - (2\eta+1)\ln 2]/(\eta+1)^2$$

and δ is the density effect correction[13-16], which for Si absorber and for $1.26 < \beta\gamma < 1000$ is

$$\delta = 4.606 \log_{10}(\beta\gamma) - 4.38 + 0.0874(3 - \log_{10}(\beta\gamma))^{3.586} .$$

In the Landau theory, the most probable collision loss, ε_{mp}, is related to the mean collision-loss (see Appendix 1 of Ref.(1)) and is independent of the mass of the incoming particle[17]

$$\varepsilon_{mp} = \xi(0.198 + \beta^2 + \ln(\xi/E_M) + \langle\varepsilon\rangle/\xi) \qquad (7)$$

where $\langle\varepsilon\rangle = (d\varepsilon/dx)x$ (for a small path length), E_m[18] is the maximum amount of energy transferred to an atomic electron in a single collision.

From eqs.(6) and (7) and for relativistic electrons, like those selected from the Ru source in this experiment, we have

$$\varepsilon_{mp} \approx 0.199x(17.451 + \ln(x)) \qquad \text{(MeV)} . \qquad (8)$$

This formula, averaged over $0.92 < \beta < 0.99$, is valid within a 7%.

4.2.- Energy-loss measurements of the active layer

Data samples of about 30000 events have been taken at different applied reverse biases (V) corresponding to the depleted layers (X_d) given in Table I for detector N6 and in Table II for detector A. In both cases the largest width of the field free region X_{FF} was about 180 μm. In this way the correction due to the ln(x) departure from linearity of the most probable energy-loss (eq.(8)) does not exceed the 4%. The data were taken for shaping times of 0.5, 1.0 and 2.0 μs ($X_M = X_{0.5}$, X_1 and X_2, correspondingly).

TABLE I - Detector N6

Capacitance (C), depleted layer (X_d) and migrating contribution values $X_M=X_2$, X_1, $X_{0.5}$ vs applied reverse bias (V); X_{FF} is the field-free layer.

V V	C pF	X_d µm	X_2 µm	X_1 µm	$X_{0.5}$ µm	X_{FF} µm
99.0	27.7±0.2	383±3				
53.9	31.4±0.2	330±2	40.9±2.7	27.6±2.6	18.7±1.8	53±2
39.3	35.8±0.2	290±2	59.1±4.0	26.5±2.5	12.2±1.2	93±2
29.4	40.9±0.2	254±1	56.8±3.8	30.4±2.9	14.6±1.4	129±1
24.5	44.7±0.2	232±1	55.6±3.7	26.1±2.5	11.5±1.1	151±1
19.5	50.1±0.2	207±1	54.2±3.6	23.7±2.3	8.8±0.8	176±1

TABLE II - Detector A

Capacitance (C), depleted layer (X_d) and migrating contribution values $X_M=X_2$ vs applied reverse bias (V); X_{FF} is the field-free layer.

V V	C pF	X_d µm	X_2 µm	X_{FF} µm
78.7	24.8±0.2	419±3		
12.7	28.3±0.2	366±3	49.9±3.6	53±3
9.3	31.2±0.2	332±2	72.0±4.8	87±3
8.3	32.8±0.2	316±2	60.8±4.0	103±2
6.8	35.7±0.2	291±2	52.3±3.5	128±2
5.4	39.7±0.2	261±1	51.5±3.5	158±1
4.4	43.1±0.2	241±1	60.4±4.1	178±1

The experimental energy-loss distributions for each depleted layer depth were fitted to the Landau probability density convolved with a Gaussian with free parameters[19] $\sigma = \sqrt{(\sigma^2_{noise}+\sigma^2_E)}$, ξ and ε_{mp}. The fitting procedure is described in Ref.(9). The good fits obtained give confidence in the appropriateness of the procedure. In order to avoid systematic errors in evaluating X_M, the energy loss upper limits (to which the experimental distributions of the fully depleted detectors were fitted) have been varied.

In Figs. 4 and 5, the energy-loss spectra sensed by the detector N6 are shown. The full lines are the fitted functions. In Figs. 6 and 7 the same as in Figs. 4 and 5 but for detector A.

Generally the fits had probabilities of 60% or better and the errors on the ε_{mp} values were about 1%. In the X_M computation, the dominant contribution to the overall error comes from the approximation of eq.(8).

At each value of the applied reverse bias, the field free contribution to the overall sensitive layer (X_M+X_d) was calculated by solving

$$\varepsilon_{mp}(X_M+X_d)/\varepsilon_{mp}(X_{fd}) \approx (X_M+X_d)/X_{fd}$$

$$\left[17.451+\ln(X_M+X_d)\right] / \left[17.451+\ln(X_{fd})\right]$$

where X_d and X_{fd} are the actual depleted layer and the fully depleted layer correspondingly; $\varepsilon_{mp}(X_M+X_d)$ and $\varepsilon_{mp}(X_{fd})$ are the corresponding values of the most probable energy-loss.

4.3.- Expected migration effect and discussion

The electron-hole pairs produced subsequently to the passage of a relativistic particle are about 80-90 μm^{-1}. They are not localized along the particle path, but spread out due to the soft δ-rays emitted in the collision loss process. The initial cylinder containing the pairs has a radius of about 2-3 μm. Thus during the first 10 ns (or less) after the passage of the particle, the minority carrier concentration is high enough to allow the diffusion coefficient to be replaced by the ambipolar diffusion coefficient.

A Monte Carlo simulation of the charge migration for an n-type bulk detector has been performed[20] considering collection times between 0.1 and 2.0 μs.

In Fig. 8, the expected contributions from the field free region to the overall sensitive layer are shown as a function of the available extension of the field free region, X_{FF}, and the collection time. The maximum field free contribution F, i.e. when it becomes independent of X_{FF} is

$$F \approx (2/5)\sigma_M \qquad (9)$$

where $\sigma_M = (\sqrt{2\tau D_p})+\sqrt{(2\tau D_n)}) \approx 13.3\sqrt{\tau}$, is the collection time.

The experimental values of X_M, for the detector N6 are shown in Fig. 9. The dashed lines are the expected values for effective collection times of 1.09, 0.25 and 0.05 μs respectively (the data are for electronics shaping times of 2.0, 1.0 and 0.5 μs). These times are obtained by solving eq.(9) and assuming that for $X_{FF} > 100$-150 μm the saturation region, visible in Fig.8, is already reached. The values of X_M are given in Tables I and II for the detectors N6 and A. The X_M data for the detectors N6 and A taken with the same shaping time (2 μs) show an agreement as a function of the field free region width X_{FF}.

The ratio of the square root of these effective collection times (such as $\sqrt{1.05}/\sqrt{0.25}$ or $\sqrt{0.25}/\sqrt{0.05}$) is approximatly equal to the corresponding ratio of the shaping times of the electronics

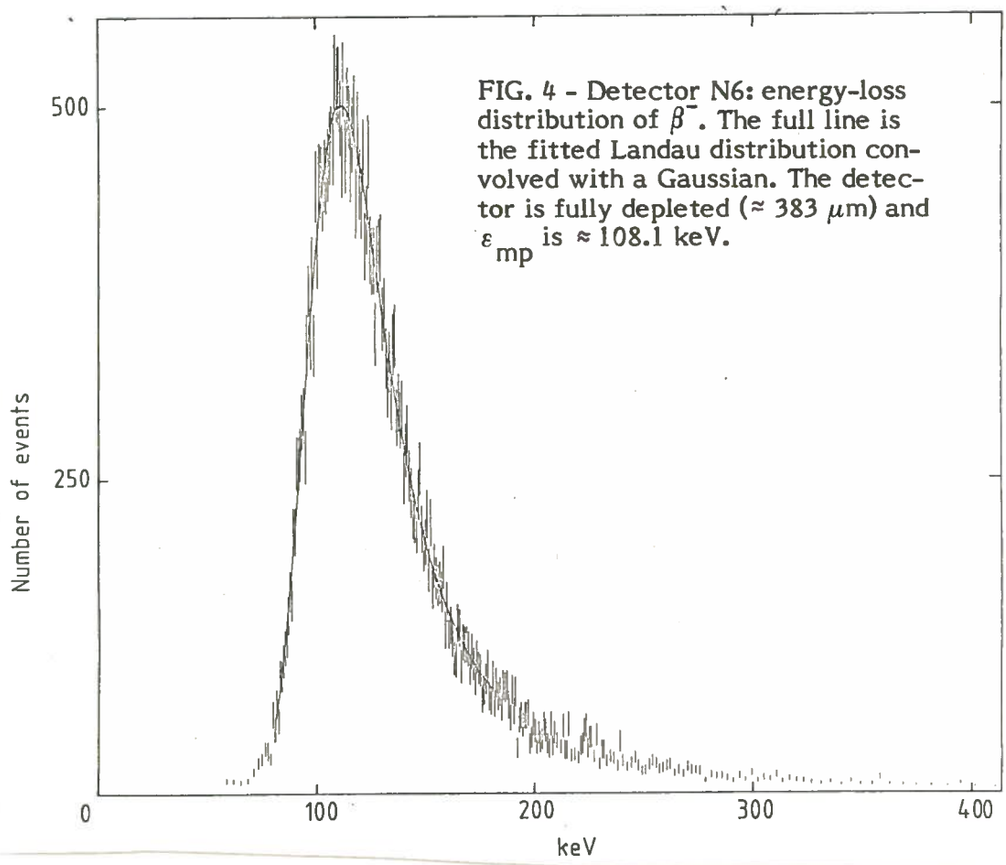

FIG. 4 - Detector N6: energy-loss distribution of β^-. The full line is the fitted Landau distribution convolved with a Gaussian. The detector is fully depleted ($\approx$ 383 μm) and ε_{mp} is $\approx$ 108.1 keV.

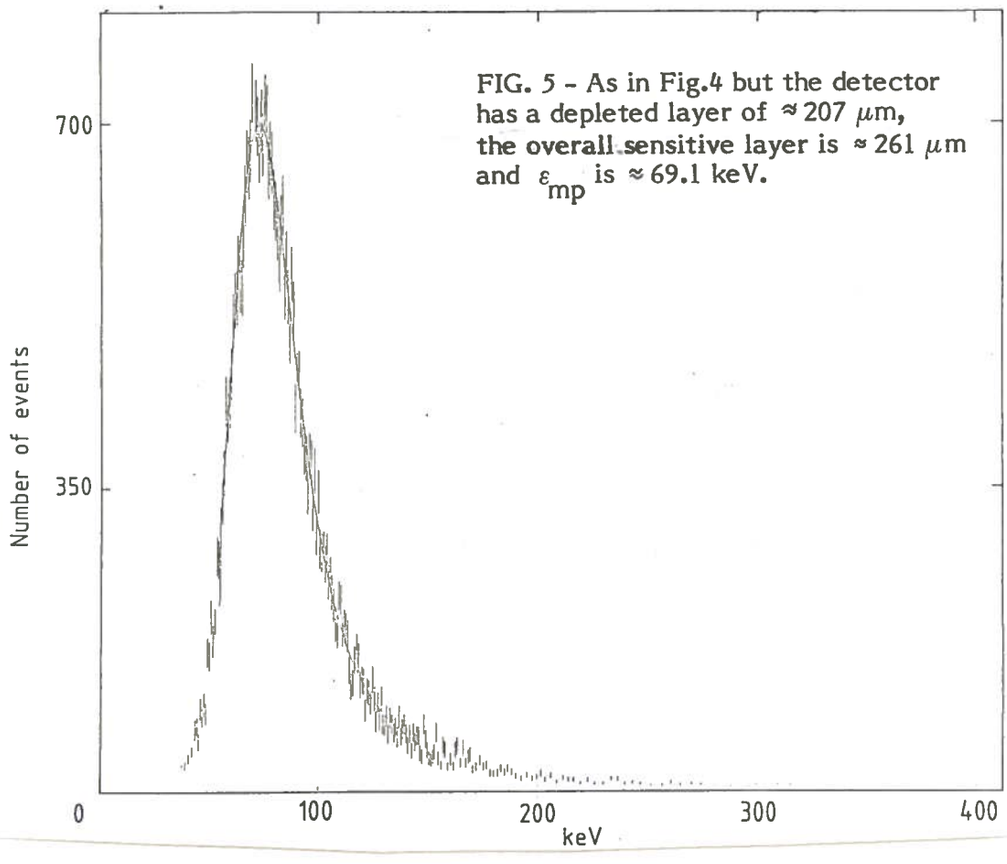

FIG. 5 - As in Fig.4 but the detector has a depleted layer of $\approx$ 207 μm, the overall sensitive layer is $\approx$ 261 μm and ε_{mp} is $\approx$ 69.1 keV.

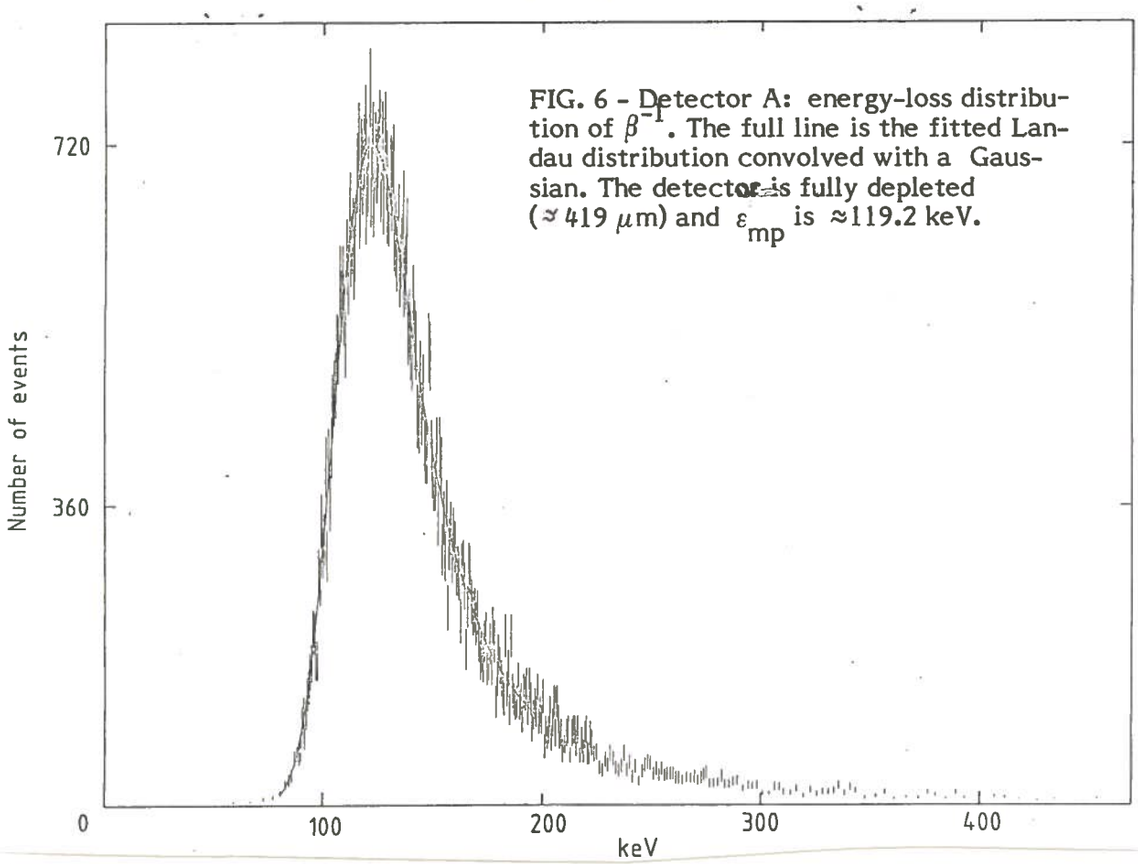

FIG. 6 - Detector A: energy-loss distribution of β^{-1}. The full line is the fitted Landau distribution convolved with a Gaussian. The detector is fully depleted ($\simeq 419\ \mu$m) and ε_{mp} is ≈ 119.2 keV.

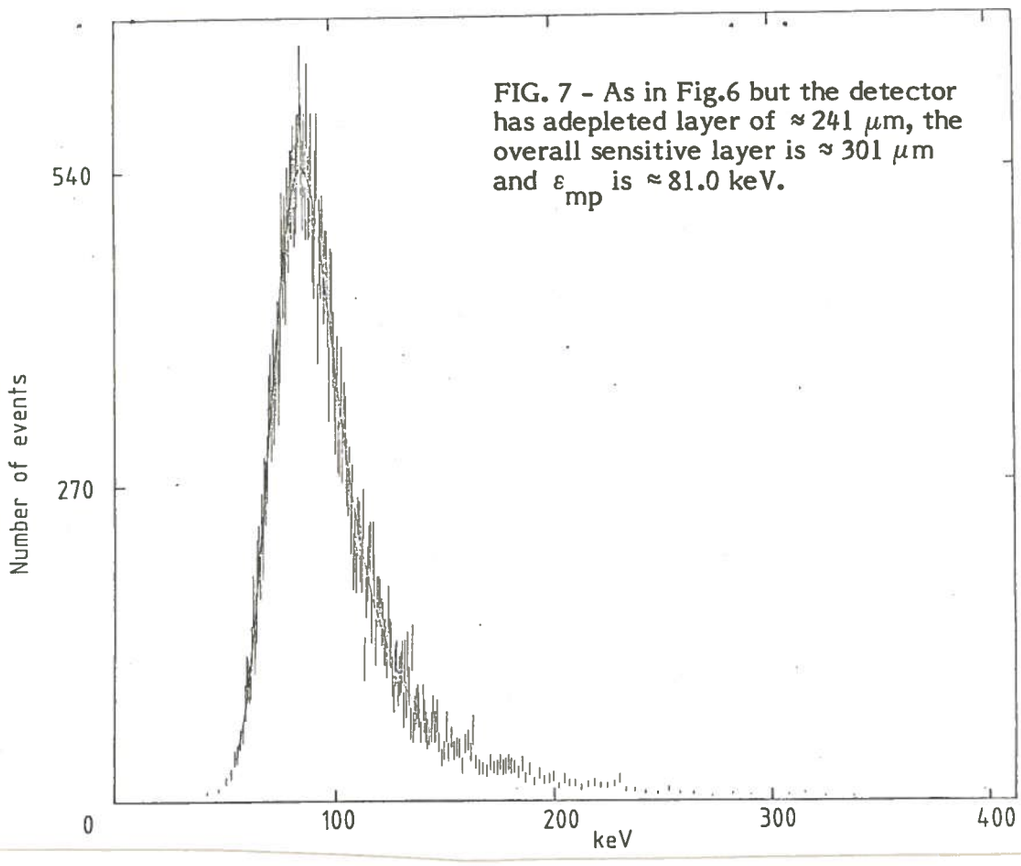

FIG. 7 - As in Fig.6 but the detector has adepleted layer of $\approx 241\ \mu$m, the overall sensitive layer is $\approx 301\ \mu$m and ε_{mp} is ≈ 81.0 keV.

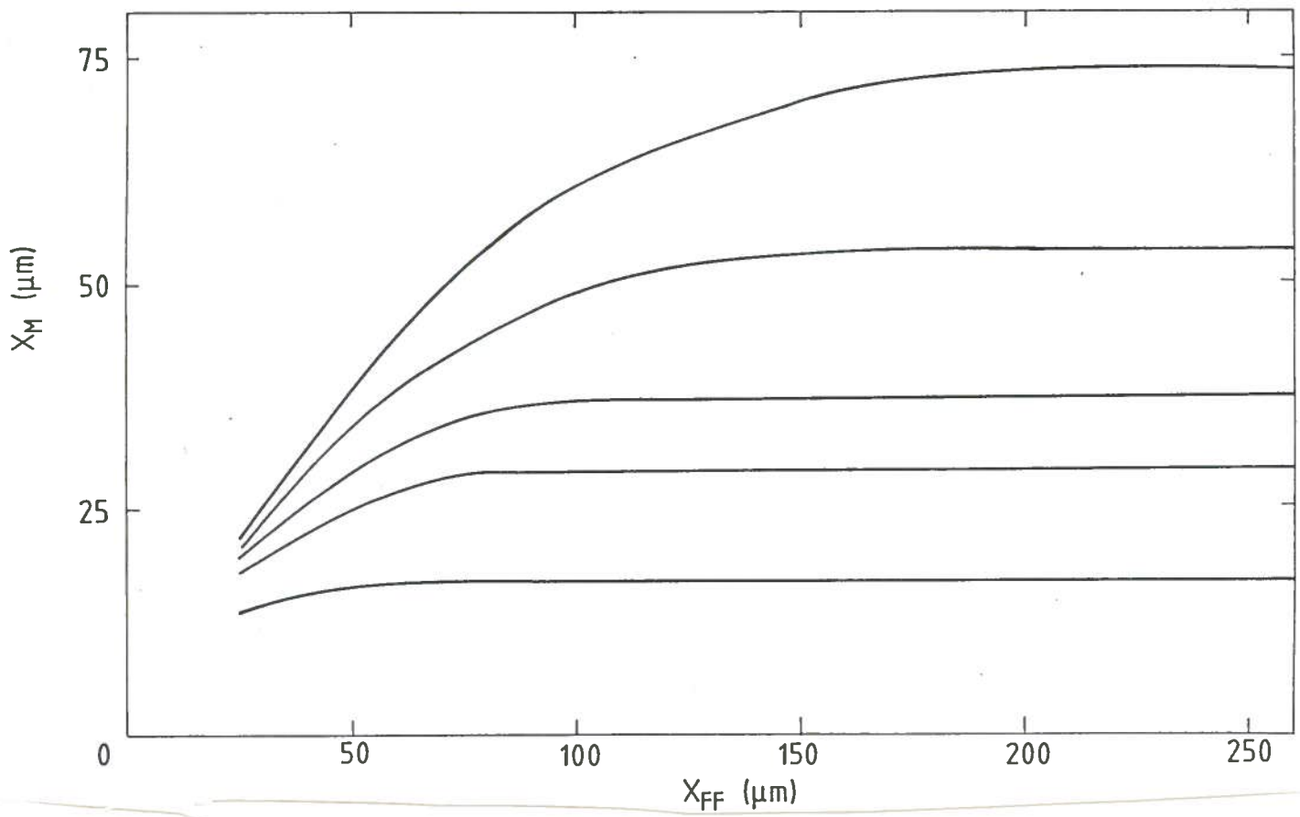

FIG. 8 - Expected contribution, X_M, to the overall sensitive layer due to charge migration as a function of the extension of the free field region X_{FF}. The collection times are (from the top) 2.0, 1.0, 0.5, 0.3 and 0.1 μs.

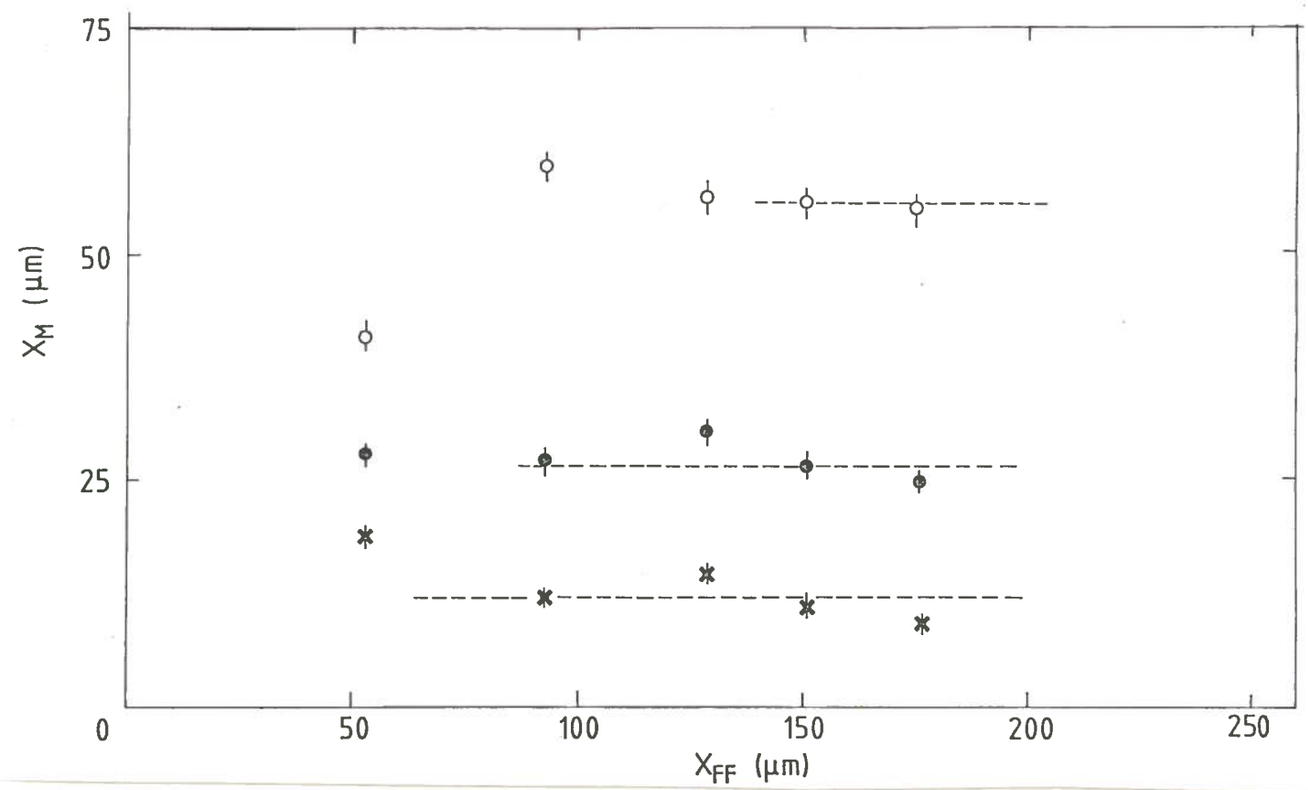

FIG. 9 - Experimental values of X_M at 2.0 μs (o), 1.0 μs (•) and 0.5 μs (x) of the shaping time. The dashed lines are (from the top) the F values (eq.(9)) for 1.09, 0.25 and 0.05 μs of effective collection time.

(namely 2.0/1.0 or 1.0/0.5). In fact the output pulse from the differentiating stage of 472 spectroscopy amplifier is expected to be proportional to the derivative of the input signal and to the shaping time, when the latter is not much greater any more than the collection time. This happens especially for the signal due to the charge migration effect. Thus varying the shaping time of the 472 spectroscopy amplifier means to vary quadratically the effective collection time.

5.- CONCLUSION

The charge migration from the field free region was detected. Both electrons and holes contribute to the net charge migration. This agrees with the prediction of a model which does not take into account recombination. For field-free region, X_{FF}, greater than 100-200 μm the overall sensitive layer becomes independent of X_{FF} and is about $(2/5)\sigma_M$.

In undepleted detectors, coupled with long integrating electronics, like those suggested for calorimetric applications in high energy physics, the contribution from the field free region to the overall sensitive layer is not negligible.

ACKNOWLEDGMENTS

The authors are indebted to the Staff of the CERN E.A. group and of Tel-Aviv University for the collaboration in preparing the experimental test.

REFERENCES AND FOOTNOTES

(1) - P.G.Rancoita and A.Seidman, Riv. Nuovo Cimento 5, no. 7 (1982).

(2) - P.G.Rancoita, Silicon detectors and elementary particle physics, Report INFN/AE-83/7 (1983), Journal of Physics G10, 299 (1984).

(3) - P.G.Rancoita, U.Koetz, R.Klanner and H.Lierl, Proceedings of the Workshop on Experimentation at HERA machine, Amsterdam, June 1983, DESY HERA 83/20 (1983), p. 105.

(4) - G.Barbiellini, G.Cecchet, J.Y.Hemery, F.Lemeilleur, P.G.Rancoita, A.Seidman and M.Zilka, Silicon/tungsten calorimeter as luminosity monitor, contributed paper no. 102 to the Intern. Europhysics Conf. on High Energy Physics, Brighton, July 1983; Report INFN/TC-83/15 (1983).

(5) - P.G.Rancoita and A.Seidman, Silicon detectors in calorimetry, Report INFN/AE-84/1 (1984), to appear in Nuclear Instr. and Meth.

(6) - The diffusion coefficient is given by the Einstein relationship

$$D = kT\mu/e$$

where k is the Boltzmann constant, T is the absolute temperature, μ is the carrier mobility and e is the charge of the electron.

(7) - For high-resistivity silicon τ_c is of the order of hundreds μs and the collection-time τ, several μs.

(8) - The N6 detector was manufactured by Micron Semiconductors (U.K.) and the A detector by Enertec (F).

(9) - S.Hancock, F.James, J.Movchet, P.G.Rancoita and L.Van Rossum, Phys. Rev. A28, 615 (1983).

(10) - The ln(x) correction to the linear dependence on the traversed thickness x of the most probable energy-loss has been calculated for this experiment and presented in this chapter.

(11) - M.J.Berger and S.M.Seltzer, Studies in penetration of charged particles in matter, Pub. 1133 Nat. Acad. of Scien.-Nat. Res. Counc. (Washington, 1964), p. 206.

(12) - F.Rohrich and B.C.Carlson, Phys. Rev. 93, 38 (1954).

(13) - R.M.Sternheimer, Phys. Rev. 117, 485 (1960).

(14) - R.M.Sternheimer, Phys. Rev. 145, 247 (1966).

(15) - R.M.Sternheimer, Phys. Rev. B3, 3681 (1971).

(16) - R.M.Sternheimer, Density effect for the ionization loss of charged particles in various substances, Report BNL-33571 (1983).

(17) - R.M.Sternheimer, Meth. of Exp. Phys., Ed. by L.Marton (Academic Press, 1961), Vol. 5A, p. 18.

(18) - E_m is given by

$$E_m = 2m_e c^2 \beta^2 \gamma^2 \left[1+(2\gamma m_e/m)+(m_e/m)^2\right]^{-1}$$

where m is the mass of the incoming particle.

(19) - The quantity σ_E takes into account the effect of atomic electron binding energies[9] and σ_{noise} is the standard deviation of the noise gaussian distribution, measured independently for each data taking.

(20) - The detector size has been assumed to be 1 cm^2. The beam was supposed to be normal to the detector surface and to traverse its middle.